Observation of strong leakage reduction in crystal assisted collimation of the SPS beam

W. Scandale,[1,2,5] G. Arduini,[1] M. Butcher,[1] F. Cerutti,[1] M. Garattini,[1] S. Gilardoni,[1] A. Lechner,[1] R. Losito,[1] A. Masi,[1] A. Mereghetti,[1] E. Metral,[1] D. Mirarchi,[1,10] S. Montesano,[1] S. Redaelli,[1] R. Rossi,[1,5] P. Schoofs,[1] G. Smirnov,[1] E. Bagli,[3] L. Bandiera,[3] S. Baricordi,[3] P. Dalpiaz,[3] G. Germogli,[3] V. Guidi,[3] A. Mazzolari,[3] D. Vincenzi,[3] G. Claps,[4] S. Dabagov,[4,11,12] D. Hampai,[4] F. Murtas,[4] G. Cavoto,[5] F. Iacoangeli,[5] L. Ludovici,[5] R. Santacesaria,[5] P. Valente,[5] F. Galluccio[6] A.G. Afonin,[7] Yu.A. Chesnokov,[7] A.A. Durum,[7] V.A. Maisheev,[7] Yu.E. Sandomirskiy,[7] A.A. Yanovich,[7] A.D. Kovalenko,[8] A.M. Taratin,[8] Yu.A. Gavrikov,[9] Yu.M. Ivanov,[9] L.P. Lapina,[9] J. Fulcher,[10] G. Hall,[10] M. Pesaresi,[10] M. Raymond,[10]

[1]CERN, European Organization for Nuclear Research, CH-1211 Geneva 23, Switzerland
[2]Laboratoire de l'Accelerateur Lineaire (LAL), Universite Paris Sud Orsay, Orsay France
[3]INFN Sezione di Ferrara, Dipartimento di Fisica, Università di Ferrara, Ferrara, Italy
[4]INFN LNF, Via E. Fermi, 40 00044 Frascati (Roma) Italy
[5]INFN Sezione di Roma, Piazzale Aldo Moro 2, 00185 Rome, Italy
[6]INFN Sezione di Napoli, Italy
[7]Institute of High Energy Physics, Moscow Region, RU-142284 Protvino, Russia
[8]Joint Institute for Nuclear Research, Joliot-Curie 6, 141980, Dubna, Moscow Region, Russia
[9]Petersburg Nuclear Physics Institute, 188300 Gatchina, Leningrad Region, Russia
[10]Imperial College, London, United Kingdom
[11]RAS P.N. Lebedev Physical Institute, Moscow, Russia
[12]NR Nuclear University MEPhI, Moscow, Russia

Abstract

In ideal two-stage collimation systems, the secondary collimator-absorbers should exclude the exit of primary particles with large impact parameters. A strong reduction of leakage for channeling conditions has been observed in the crystal-assisted collimation of the SPS beam of 270 GeV/c protons, approaching the ideal conditions.

Keywords: accelerator, beam collimation, crystal, channeling.

PACS numbers: 29.27.-a, 61.85.+p

1. Introduction

A multi-stage collimation system is used in the Large Hadron Collider (LHC) to absorb halo particles of the circulating beam [1]. A crystal-assisted collimation scheme for LHC is presently under study [2]. A bent crystal used as a primary collimator instead of a bulk target deflects halo particles in the channeling regime, directing them into one single secondary collimator-absorber potentially at larger transverse apertures than the secondary collimators of the classic multi-stage system.

Fig. 1 shows the distributions of the impact parameters of protons with the absorber obtained by simulation, which should be realized in the experiment discussed below on crystal assisted collimation of the Super Proton Synchrotron (SPS) proton beam. In the case of crystal orientation optimal for channeling (2), the halo fraction, which hits the absorber edge, is considerably smaller than in the case of an amorphous crystal orientation (1). As a result, the number of particles returning back into the beam due to scattering at the surface of the absorber should be strongly reduced, thus increasing the collimation efficiency. The first experiments on crystal assisted collimation were performed at the IHEP synchrotron [3], RHIC [4] and Tevatron [5].

The UA9 experimental studies [6-9] on crystal assisted collimation of the SPS beam which started a few years ago showed that crystal alignment with the circulated beam halo could be obtained quickly using the beam loss monitors (BLM_1) installed downstream of the crystal, as shown by the schematic layout in Fig. 2. Channeled particles with small oscillation amplitudes in the crystal planar channels do not have close collisions with the crystal nuclei, and, consequently, do not experience nuclear interactions. Therefore, the beam losses in the aligned crystal are strongly decreased compared to the case when the crystal is in amorphous orientation.

In our previous experiments, the collimation leakage was measured by the monitor BLM_2 installed in the first high dispersion (HD) area downstream of the collimator-absorber where off-momentum particles produced in the collimation area have the first possibility to hit the beam pipe. A considerable reduction of the collimation leakage was always observed for the channeling orientation of a crystal. For the case of an SPS beam of Pb ions with 270 GeV/c momentum per unit charge, the loss reduction observed in the HD area by BLM_2 is practically the same as in the crystal because the probability of backscattering from the tungsten absorber is very small for Pb ions due to their high probability of nuclear

interactions. In the case of protons, the beam loss reduction detected by BLM_2 was always smaller than in the crystal because of the contribution of particles emerging from the absorber [8]. [I did not find the previous sentence too clear and presume that it refers to BLM_1 when talking about loss reduction in the crystal. If so, I think it would be clearer to make this explicit.]

In the UA9 experiments, a 60 cm long tungsten bar is used as a secondary collimator-absorber. It is insufficient for the full absorption of the halo protons. The nuclear inelastic cross-section for 270 GeV/c protons in tungsten σ_{in} = 1.725 b [10] [units are not generally italicized, although this might be dealt with by the journal] and the interaction length S_{in}=9.18 cm corresponds to the attenuation probability of the proton beam $P_{in}=exp(-L/S_{in})=1.45\times10^{-3}$. Besides, protons after losing a small part of their momentum by diffractive scattering can also remain in the beam. Protons deflected by a crystal deeply into the absorber but emerging from it with some momentum loss do not allow the observation of the collimation leakage reduction, which should occur in the case of full absorption (i.e stopping in the absorber). [This is not very clear to me. If I understand correctly, I would suggest to phrase the above as "The imperfect absorption of the tungsten target leads to an underestimation of the collimation cleaning theoretically achievable with a crystal based system, partly explaining previous discrepancies between measured and predicted performance [ref]." The last comment could also be skipped.]The situation may be considerably improved already with a 1 m long tungsten absorber, $P_{in}=1.86\times10^{-5}$

Simulation of the crystal assisted collimation of the SPS beam halo with a SixTrack code and real beam pipe aperture [14] allowed detecting the azimuth [this is unclear. I do not think the azimuth was detected but do you mean 'detection at the azimuth"?] in the first high dispersion area where the loss reduction for the crystal channeling orientation is considerably larger than that observed in the position of BLM_2. Beam loss monitors have been installed at this azimuth, BLM_3 in Fig. 2.

In this paper the results of the experiment on the crystal assisted collimation of the CERN SPS beam where the collimation leakage reduction observed with BLM_3 is considerably larger than the loss reduction in the crystal are described. The situation is close to the ideal case when full absorption of particles with large impact parameters occurs in the secondary collimator.

2. The experiment description

Figure 2 shows the schematic layout of the UA9 experiment with only those devices used in the present measurements. The crystal primary collimator and the secondary collimator-absorber (TAL) are installed at the SPS azimuths with relative horizontal betatron phase advance close to 90 degrees and with a large value of the horizontal beta function. The silicon strip crystal C1 produced using techniques described in [11,12] was used as a primary collimator. The crystal parameters are presented in Table 1. The crystal miscut angle between the crystal surface and the (110) crystallographic planes is about 10 μrad, which is much smaller than for the crystals used in our earlier experiments. This feature helps to reduce the particle losses at the crystal channeling orientation. Protons from the SPS beam halo hit the crystal and secondary particles produced in nuclear inelastic interactions are detected in the beam loss monitor BLM_1. The goniometer produced by IHEP allows adjusting the crystal orientation relative to the beam halo direction with an angular accuracy of about ±10 μrad.

Downstream of the absorber TAL there is the first high dispersion area. Off-momentum particles with momentum p and sufficiently large $\delta = p/p_o - 1$, where p_o is the momentum of the synchronous particle, emerging from either the crystal or the absorber have displacements from the orbit here, $x_\delta = D_x\delta$, where D_x is the dispersion function, and, hence, they might be lost. The targets limiting the accelerator aperture installed in the HD area were not used in this experiment. The beam loss monitor BLM_2 used in our previous experiments [8,9] detected secondary particles generated by protons in the pipe walls. One more beam loss monitor BLM_3 has been installed upstream of the quadrupole QF4. Figure 3 shows the dispersion function change in the collimation area and in the first HD area downstream of the absorber. The positions of the monitors BLM_2 and BLM_3 are close to the first and the second dispersion maxima, respectively. Additionally, it is shown that the betatron phase advance between the absorber TAL and the monitor BLM_2 equals approximately 90°. It is very important circumstance that proves the fact that protons strongly scattered in the TAL acquire a maximal betatron deviation from the orbit near BLM_2. [Not quite sure I have understood this but, if so, my suggestion would be “It is very important that protons strongly scattered in the TAL should acquire a maximal betatron deviation from the orbit near BLM_2.”]

In the SPS, the beam of protons is accelerated to 270 GeV/c with nominal betatron tunes Q_H=26.13 and Q_V=26.18. In the position of the monitor BLM_3 the beam losses are small. Therefore, a beam consisting of 12 bunches with a total intensity of 1.3×10^{12} protons was used in this experiment. The relevant accelerator parameters at the azimuths for several UA9 elements are listed in Table 2, where β_x is the horizontal beta-function, σ_x is the RMS value of

the horizontal beam size (here for the RMS emittance ε=0.009 μm·rad), and $\Delta\mu_x$ is the horizontal phase advance between the elements.

3. Experimental results

At the beginning of the measurement the two-sided collimator COL was centered relative to the closed orbit. The collimator half gap $X_{1/2}$ determined the reference beam envelope that the crystal is then aligned to. Then the alignment positions for the crystal CR1 and the absorber TAL were determined by fixing their positions at the edge of the collimator shadow. After that the crystal and the absorber were placed at a distance X_{Cl}=4.07 mm (5.17 σ_x) and X_{TAL}=7.05 mm (7.94 σ_x) from the orbit, respectively. Hence, the TAL offset relative to the crystal was X_{off}=3.06 mm. Under these conditions a scan of the horizontal angular positions of the crystal was performed with the goniometer. Figure 4a shows the dependence of beam losses in the crystal observed with BLM_1 (curve 1). The left minimum corresponds to the crystal orientation optimal for channeling where the beam losses occur mainly due to the non-channeled fraction. The ratio of the beam losses at the amorphous and channeling orientations of the crystal determines the beam loss reduction R_{bl}. The reduction measured for the area behind the crystal is $R_{bl}(1)$=11.8.

The angular region in Fig. 4 with reduced losses on the right of the channeling minimum is due to volume reflection (VR) of particles by bent crystal planes, which allows them to reach the TAL aperture in a smaller number of passages through the crystal than occurs due to multiple scattering for amorphous crystal orientations. The second minimum in the VR region observed also in our previous experiments [7,8] is clearly seen here. This minimum is observed at an angular distance from the channeling orientation equal about the crystal bend angle. As already explained [6], in this case the whole VR region is on the same side of the beam envelope direction. Therefore, angular kicks due to VR always increase the oscillation amplitudes of particles, and they more quickly reach the absorber.

Curve 2 shows the dependence of nuclear inelastic interaction number in the crystal on its orientation obtained by simulation of the collimation process with the detailed calculation of particle trajectories in the crystal, see [13]. Linear 6-D transfer matrices M(6,6) were used to transport SPS particles. The simulation for a given particle is stopped when it hits the TAL or when an inelastic interaction occurred in the crystal. The calculated dependence describes well both the width and the shape of the experimental dependence but gives smaller values of the beam losses for the channeling as well as the VR orientations of the crystal. The distributions of impact parameters of protons with the TAL obtained by simulation for some

amorphous crystal orientation (1) and for the aligned case (2) are shown in Fig. 1. Protons deflected by the crystal in the channeling regime hit the TAL at a distance of about 8 mm from its edge.

Curve 3 shows the simulation results obtained by using the SixTrack code to transport particles in the SPS. The process of diffractive scattering of protons in the crystal and TAL is taken into account [reference]. The interaction of protons with the crystal is modeled as described in [14]. considered using approximations for different processes described in [14]. In this case, the calculated width of the angular dependence is smaller than in the experiment because of the approximations used for the description of the proton interactions with the crystal. However, the loss value in the VR region is in better agreement with the experiment. The contribution of diffraction-scattered protons in repeated passages through the crystal may explain the losses in this VR region.

The beam loss reduction observed in the HD area with the monitor BLM_2 was $R_{bl}(2)=8.3$, which is considerably smaller than behind the crystal as in our previous experiments. Figure 4b shows the beam loss dependence on the crystal orientation observed in the new position with the monitor BLM_3. The angular dependence is the same as behind the crystal but the beam loss reduction in channeling is considerably larger, $R_{bl}(3)=18.1$, which is in good agreement with the simulation prediction mentioned above. The large reduction of collimation leakage is possible because the majority of channeled particles are deflected by the crystal deeply inside the TAL and, emerging from it, are significantly reduced in number for impact on BLM_3.

The particles are lost at the beam pipe near the first dispersion maximum where the betatron phase advance from the TAL exit is about 90°. Actually, the RMS deflection due to multiple Coulomb scattering in the TAL, taking into account nuclear elastic scattering, is large, $\theta_{ms}=0.742$ mrad, and the average ionization losses are estimated to be $\delta=-7.62\times10^{-3}$. The betatron amplitudes for protons deflected by the crystal in the channeling regime are about 15 mm at the TAL entrance face. At the TAL exit, protons deflected through θ_{ms} due to multiple scattering will have an amplitude of $X_m=68.6$ mm, while the amplitude near the quadrupole QF3 will be $X_m=75$ mm. Besides, the average shift near QF3 for these particles due to high dispersion is $X_\delta=\delta D_x=-28.75$ mm. The horizontal and vertical dimensions of the SPS beam pipe in the focusing quadrupoles QFs are 76 mm and 19.15 mm, respectively. The simulations show that a larger fraction of particles deflected by the crystal but which avoided absorption in the TAL should be successfully lost in this part of the pipe.

4. Conclusions

The position selected for the beam loss monitor downstream the collimation area helps to reduce considerably the contribution of particles deflected by the crystal in channeling regime but emerging from the secondary collimator-absorber. This recent change of the UA9 SPS layout, triggered by simulations indicating the role of imperfect TAL absorption on crystal-collimation cleaning, allowed observation of a strong leakage reduction of halo protons from the SPS beam collimation area, thereby approaching the case with an ideal absorber.

Acknowledgements

We wish to acknowledge the strong support of the CERN EN-STI and BE-OP groups. We also acknowledge the partial support by the Russian Foundation for Basic Research Grants 05-02-17622 and 06-02-16912, the RF President Foundation Grant SS-3383.2010.2, the ‘‘LHC Program of Presidium of Russian Academy of Sciences’’ and the grant RFBR-CERN 12-02-91532. G.Cavoto and F.Iacoangeli acknowledge the support from ERC Ideas Consolidator Grant n. 615089 "CRYSBEAM". S. Dabagov acknowledges the support by the Ministry of Education and Science of RF in the frames of Competitiveness Growth Program of NRNU MEPhI, Agreement 02.A03.21.0005. Work supported by the EuCARD program GA 227579, within the "Collimators and Materials for high power beams" work package (Colmat-WP). The Imperial College group gratefully acknowledges support from the UK Science and Technology Facilities Council.

References

[1] R. Assmann et al,, ”Requirements for the LHC Collimation System”. LHC-PROJECT-REPORT-599. 8th European Particle Accelerator Conference: A Europhysics Conference, La Vilette, Paris, France, 3-7 Jun 2002.

[2] R. Assmann, S. Redaelli, W. Scandale, in: EPAC Proceedings, Edinburgh, 2006, p.1526.

[3] A.G. Afonin et al., Phys. Rev. Lett. 87 (2001) 094802.

[4] R.P.Fliller et al., Nucl. Instr. Meth. B 234 (2005) 47.

[5] R.A.Carrigan Jr. et al., Fermilab-CONF-06-309-AD.

[6] W.Scandale et al., Phys. Letters B 692 (2010) 78.

[7] W. Scandale et al., Phys.Letters B 703 (2011) 547.

[8] W. Scandale et al., Phys.Letters B 714 (2012) 231.

[9] W. Scandale et al., Phys.Letters B 726 (2013) 182.

[10] V. Uzhinsky, A. Galoyan. Phys. Letters B 721 (2013) 68.

[11] S. Baricordi et al., Appl. Phys. Lett. **91**, 061908 (2007).

[12] S. Baricordi et al., Journal of Physics D: Applied Physics **41**, 245501 (2008).

[13] A.M. Taratin, W. Scandale, Nucl. Instr. Meth. B 313 (2013) 26.

[14] D. Mirarchi, G. Hall, S. Redaelli, W. Scandale, Nucl. Instr. Meth. B (in press).

Figure captions

FIG. 1 (color online). The calculated distributions of impact parameters with the secondary collimator-absorber for a crystal assisted collimation of the SPS beam of 270 GeV/c protons in the case of amorphous (1) and channeling (2) orientations of the crystal.

FIG. 2 (color online). A schematic layout of the UA9 experiment. The crystal primary collimator C1 is located upstream of the quadrupole QF518 (QF1). The TAL acting as a secondary collimator-absorber is upstream of the quadrupole QF 520 (QF2). The beam loss monitor BLM_1 is used to find channeling in the crystal and BLM_2 and BLM_3 are used to detect particles leaking out from the collimation area.

FIG. 3 (color online). The dependence of the dispersion function on the distance along the collimation area and the first HD area downstream of the absorber.

FIG. 4 (color online). The results of crystal assisted collimation of the SPS beam halo of 270 GeV/c protons. Curves (1) show the dependence of beam losses observed in the crystal (a) and in the HD area with the BLM_3 monitor (b) on the angular position of the crystal C1 normalized to its value for amorphous orientation of the crystal (dot-dashed line). Curves (2) and (3) show the dependence of the number of nuclear inelastic interactions of protons in the crystal on its orientation angle obtained by simulation according to [11] and [12], respectively.

Table 1. Parameters of crystal C1

Length (mm)	Bend angle α (μrad)	Bend radius R (m)	Miscast angle θ_m (μrad)
1.87	165	11.33	10

Table 2. Relevant accelerator parameters

Parameter	C1	TAL	QF3
β_x (m)	90.945	87.660	107.023
σ_x (mm)	0.9047	0.888	0.981
$\Delta\mu_x$ from C1 (2π)	0	0.2405	0.4909
D_x (m)	-0.857	-6.8×10^{-4}	3.772

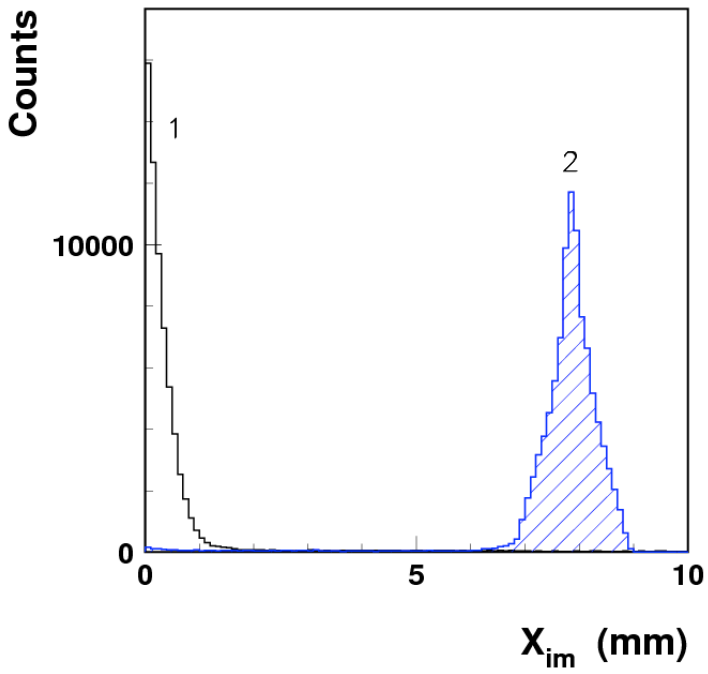

Figure 1

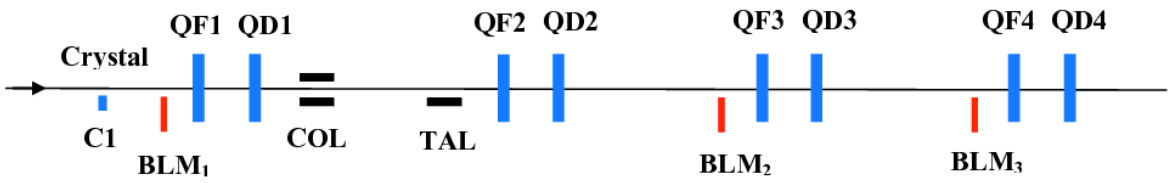
QF1
QD1
QF2
QD2
QF3
QD3
QF4
QD4
Crystal
C1
BLM1
COL
TAL
BLM2
BLM3

Figure 2

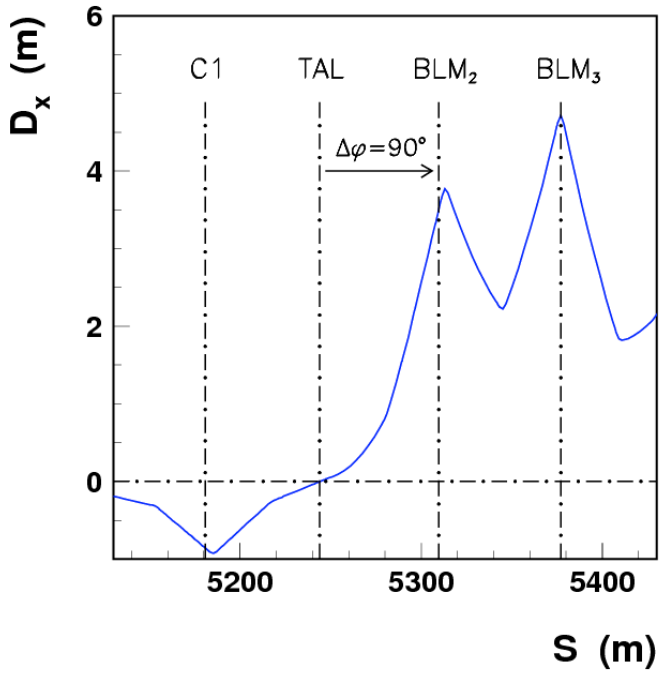

Figure 3

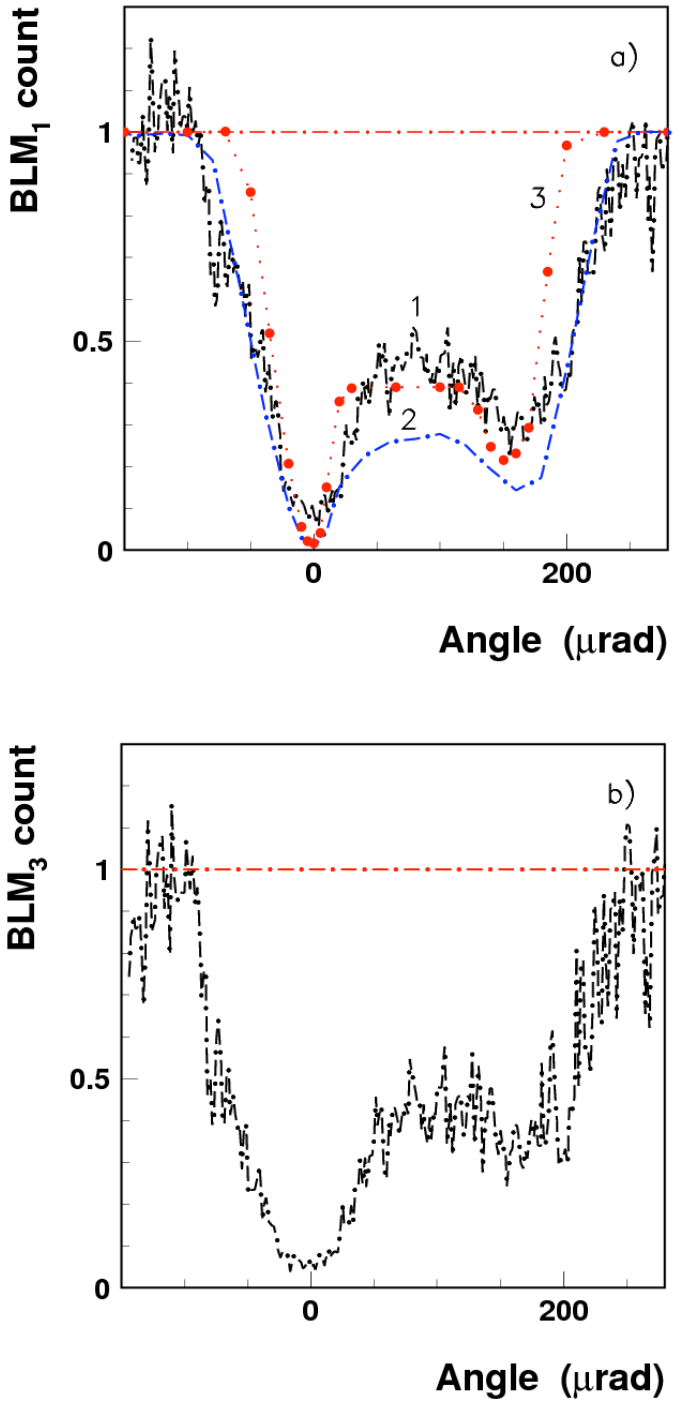
a)
BLM1 count
1
0.5
0
0
200
Angle (μrad)
1
2
3
b)
BLM3 count
1
0.5
0
0
200
Angle (μrad)

Figure 4